

Spatial Assessment of Soil Erosion in the Chitar River Basin through RUSLE–GIS Approach

Jeilani Mohammed and Shashi Mesapam
jm23cer1r14@student.nitw.ac.in, mshashi@nitw.ac.in

Department of Civil Engineering, National Institute of Technology, Warangal, Telangana – 506004, India

Keywords: Soil erosion, RUSLE model, GIS and remote sensing, spatial variability, Land use/land cover, Watershed conservation.

Abstract:

Soil erosion is a major problem, which has had adverse effects on the productivity of agriculture, the quality of water, and the sustainability of land in the long term, especially in semi-arid states of southern India. This paper examines the spatial and intensity of soil erosion in the Chitar River Basin, Tamil Nadu, through the usage of the Revised Universal Soil Loss Equation (RUSLE), the Geographic Information System (GIS) techniques and remote-sensing techniques. RUSLE components, such as rainfall erosivity (R), soil erodibility (K), slope length and steepness (LS), cover management (C), and support practices (P), were calculated based on the Indian Meteorological Department rainfall data, FAO soil data, a digital elevation model and Landsat-based land-use/land-cover data. Annual soil loss deposition ranges from negligible to over 100 t/ha/yr, confirming the basin's high spatial variability. Findings indicate that most of the basin is very low to minimal erosion (0–10 t ha⁻¹ yr⁻¹), and moderate erosion (10–25 t ha⁻¹ yr⁻¹) occurs sporadically. Spatial areas are limited to high and very severe erosion zones (25–100 t ha⁻¹ yr⁻¹) and extreme erosion areas (100 t ha⁻¹ yr⁻¹), which are mainly found in steep slopes, upper catchments and drainage networks, where high values of R, LS and C are also accompanied by relative high values of P-factor. These focal areas of erosion are a disproportionate contributor to sediment yield and thus require immediate Erosion conservation measures, including contour bunding, terraces, afforestation, and check dams. The study revealed that the RUSLE and GIS method is a highly effective instrument of defining erosion susceptible areas and the basis of managing the watersheds on a sustainable and targeted basis in the Chitar River Basin.

1. Introduction:

Soil erosion risk is widely regarded as a major environmental issue contributing to land deterioration (Aiello et al., 2015). It is a process through which the soil particles are broken loose, carried, and deposited by erosive forces including wind and water hence affecting natural productivity of agriculture, resources, and sustainability (Pimentel et al., 1995). This phenomenon reduces land fertility and crop productivity by modifying soil properties, particularly through decreased water availability, restricted infiltration, Runoff intensification from impermeable subsoil layers, fertile topsoil depletion, and depletion of essential plant nutrients (Hui et al., 2010). The biophysical environment, comprising of soil properties, climatic variables, topographic properties and vegetation covers, has a significant modulation on soil erosion. Basic topographic factors, including the slope length, aspect and landform structure, have a significant impact on the erosional processes (Ganasri.,2016). According to the report by the Centre for Soil and Water Conservation Research and Training Institute (Dogra, 2011), about 68.4% of India's eroded land area is affected by water-driven erosion, and nearly 29% of the eroded soil is transported to the sea and permanently removed (Narayana et al., 1983). The R factor is used to determine erosion-prone zones and to support the development of soil conservation plans. Topsoil is particularly susceptible to erosion because of the frequent occurrence of high-intensity rainfall with strong erosive potential (Shi et al., 2010). Direct field-based monitoring of soil erosion is time-consuming, expensive, and typically confined to limited experimental plots. Therefore, evaluating the extent of water-induced soil erosion at a national scale necessitates a comprehensive modeling framework. Several physical and empirical models have been developed to predict soil erosion by integrating GIS and remote sensing

(RS) technologies at various spatiotemporal scales (Zhang et al., 2021).

Although many physical models are used globally to estimate soil loss, their performance and applicability vary, mainly due to differences in input data requirements and modeling approaches. Models such as CREAMS, ANSWERS, EPIC, Guest, WEPP, area available to evaluate hydrology and sediment dynamics through quantitative models (Kazamias and Sapountzis, 2017). However, these models may not be suitable for large countries such as India because of substantial topographic heterogeneity and the limited availability of consistent spatiotemporal datasets (Kayet et al., 2018).

In contrast, the Universal Soil Loss Equation (USLE) (Wischmeier and Smith, 1978a,b) and its revised version, the Revised Universal Soil Loss Equation (RUSLE) (Renard et al., 1991), are empirical models that have been widely applied worldwide, including in India, to estimate long-term average annual soil erosion in small-, medium-, and large-scale watersheds due to their low data requirements and simplicity (Balasubramani et al., 2015). These techniques can be applied to produce a Soil loss susceptibility map, provide the spatial distribution of factors controlling water erosion, and the erosion risk in different areas of the catchment. It is difficult to access spatial information in the Emerging economies (Hui et al. 2010).

This study assesses soil erosion risk using the RUSLE model integrated with RS and GIS techniques. Spatial analysis of the variability of erosion-controlling factors was carried out to outline the areas that were prone to erosion. The results show that there is high water-related soil erosion and the importance of adopting strong Soil and water management interventions.

2. Study Area:

The Chitar River Basin is a sub-basin of the Thamirabarani River system, located in southern Tamil Nadu, India, extending between 8°35'–9°15' N latitude and 77°20'–77°55' E longitude, and covering an area of approximately 2,150 km² as shown in Figure 1. The sub-humid climatic regime over the basin and the topography which is heterogeneous in nature, with hilly terrain of the foothills of the Western Ghats to the downstream gently undulating plains. The gradient of elevation and slope has a strong control effect on hydrological processes especially generation of run off and erosional dynamics. The drainage system is of a dendritic to sub-dendritic pattern with the dominance of precipitation being controlled by the northeast monsoon. High seasonal precipitation also adds to overland flow-induced soil erosion.

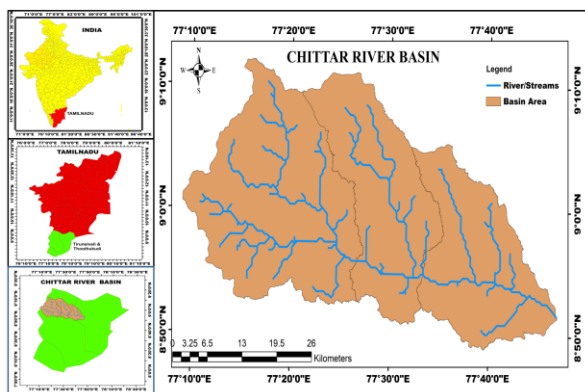


Figure 1. Study area map of the Chitar river basin

3. Materials and Methods:

3.1 Materials:

For the Chitar River Basin, Survey of India (SOI) toposheets at a scale of 1:50,000 covering the entire basin area were used for base map preparation and drainage network extraction. These toposheets were obtained from the Survey of India. Shuttle Radar Topography Mission (SRTM) Digital Elevation Model (DEM) data with a spatial resolution of 90 m were used for watershed delineation and terrain analysis. Land use/land cover (LULC) and soil maps for the study area were obtained from authorized sources. LULC features were accurately delineated through on-screen visual interpretation and digital analysis of fused satellite imagery derived from High- to coarse-resolution datasets, including Sentinel-2A. The soil map provides a geographical representation of the spatial distribution of soil types and associated soil properties within the Basin and was used for deriving soil erodibility information required for erosion modelling.

3.2 Methods

In the present study, GIS analysis was performed with ArcGIS software in conjunction with remote sensing (RS) data. The Basin was delineated from Shuttle Radar Topography Mission (SRTM) DEM data with a spatial resolution of 90 m, and the drainage network was generated using Survey of India toposheets. The Universal Soil Loss Equation (USLE) requires five parameters, namely rainfall erosivity (R), soil erodibility (K), slope length and steepness (LS), support practice (P) and cover management (C) factors.

These parameters were derived from meteorological data, field observations, and remote sensing datasets. The rainfall erosivity factor was estimated from long-term annual rainfall data using GIS-based interpolation techniques. Soil erodibility was determined from soil survey data by extracting and organic matter content and soil texture. The LS factor was generated from the DEM of the study area. Land use and land cover (LULC) information was obtained from Sentinel satellite imagery of 10 m spatial resolution, and the C and P factors were assigned based on the LULC map. The methodology adopted in the study is illustrated in Figure 2.

$$A=R*K*L*S*P*C$$

Where *A* represents the potential average annual soil loss; *R* is the rainfall erosivity factor; *K* is soil erodibility factor; *L* is the slope length factor; *S* represents the slope; *C* is the cropping management factor; and *P* denotes the support practice factor.

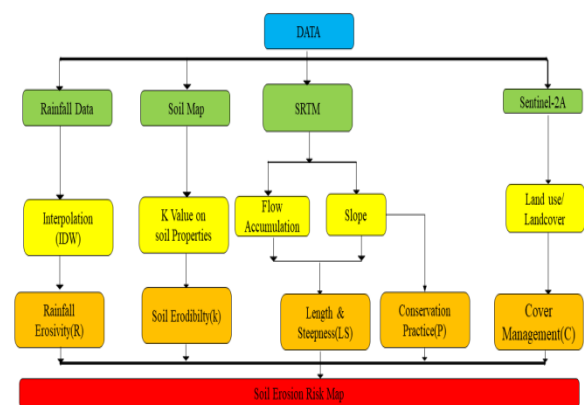


Figure 2. Methodology of study area

4. Result and Discussion:

4.1 Rainfall Erosivity:

Rainfall erosivity is an index that quantifies the erosive potential of rainfall to detach and transport soil particles. Due to the lack of hourly rainfall intensity data, monthly and annual rainfall data were used to calculate the rainfall erosivity using Wischmeier and Smith (1978) in Equation 1.

$$R = \sum_{i=1}^{12} 1.735 * 10^{(1.5 \log_{10} \left[\frac{P_i^2}{P} \right] - 0.08188)} \quad (1)$$

Where *R* is the rainfall erosivity factor (MJ.mm.ha⁻¹.h⁻¹.yr⁻¹), *P_i* is rainfall in monthly (mm), and *P* is the rainfall in annual (mm). Rainfall erosivity (R-factor) in the study basin varies from 950 to 1,150 MJ.mm.ha⁻¹.h⁻¹.yr⁻¹, indicating a moderate to high rainfall erosive potential across the area. Higher erosivity values are predominantly observed in the western part of the basin, while relatively lower values are concentrated in the central region (Mohammed et al., 2026), as illustrated in Figure 3. This spatial variation is mainly attributed to differences in rainfall intensity and distribution, where regions experiencing frequent high-intensity precipitation contribute significantly to elevated erosivity levels. The results suggest that rainfall acts as a major driving force for soil detachment and transport, particularly during

peak monsoon periods, thereby increasing the susceptibility of the basin to soil erosion. In contrast, the comparatively lower values in the central region may be due to more uniform and less intense rainfall patterns. Overall, the spatial distribution of the R-factor highlights the need for targeted soil and water conservation measures, especially in high-erosivity zones, to effectively mitigate soil erosion and promote sustainable land management practices, as shown in Figure 3a&b.

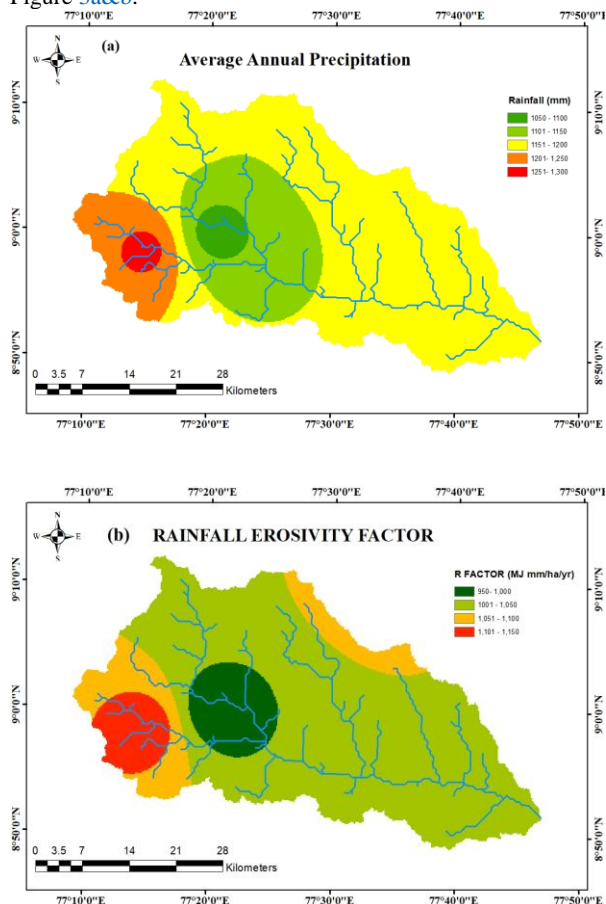


Figure 3. (a) Average Annual Precipitation, (b) Rainfall Factor Map

4.2 Soil Erodibility Factor:

Soil erodibility is one of the most critical determinants in the estimation of soil loss, as it directly reflects the susceptibility of soil particles to detachment and transport under rainfall and runoff conditions. The soil erodibility factor (K) serves as a key index for the quantitative evaluation of this susceptibility and is commonly derived using the Universal Soil Loss Equation (USLE) nomograph, which integrates soil properties such as texture, organic matter content, structure, and permeability. In the present basin, four major soil classes—clay loam, sandy loam, gravel, and clay—have been identified, each exhibiting distinct erodibility characteristics. The estimated K-values across the basin range from 0.0205 to 0.0231, indicating generally low to moderate erosion potential. Spatially, relatively higher K-values are observed in the western part of the basin, primarily due to the dominance of finer-textured and more homogeneous soils that tend to have weaker structural stability and are more prone to detachment under rainfall impact. In contrast, lower K-values are recorded in the central and eastern regions,

where soils exhibit comparatively better aggregation, permeability, or protective characteristics that reduce erosion susceptibility. This spatial variability highlights the significant role of inherent soil properties in influencing erosion processes and underscores the need to incorporate soil-specific conservation measures in erosion control planning. The distribution pattern of K-values, as illustrated in Figure 4, provides valuable insight into areas that are more vulnerable to soil loss and can aid in prioritizing appropriate soil and water conservation strategies across the basin. Furthermore, understanding these variations is essential for developing site-specific management practices and improving the accuracy of soil erosion modeling. This also supports informed decision-making for sustainable land use planning and long-term watershed management.

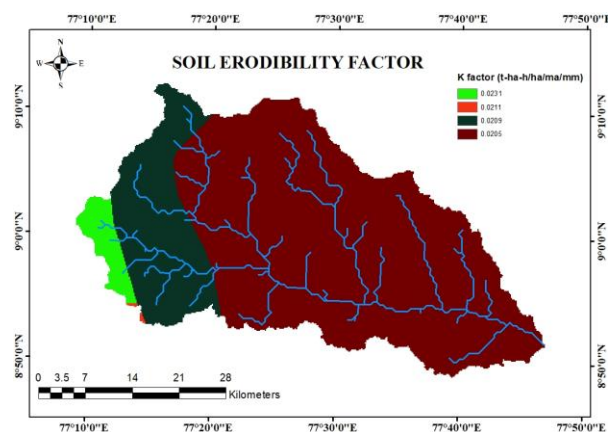


Figure 4. Soil Erodibility Factor Map

4.3 Topographic Factor (LS):

The LS factor described the product of slope length (L) and steepness slope (S) on the erosion of soil. The LS factor then measures topographic effects on erosion by explaining the recorded rise in soil loss in relation to both gradient and length. The LS factor in this study was calculated using digital elevation model data at a 90m spatial scale, where steeper and longer slopes are expected to be more likely to cause erosion. The slope length component (L) was calculated after the procedure, whereas the slope steepness component (S) was calculated as per Wischmeier and Smith (1978 a,b). The LS factor takes a measure of 0 to 178.12 indicating that there is a significant heterogeneity of the terrain conditions across the basin in Figure 5.

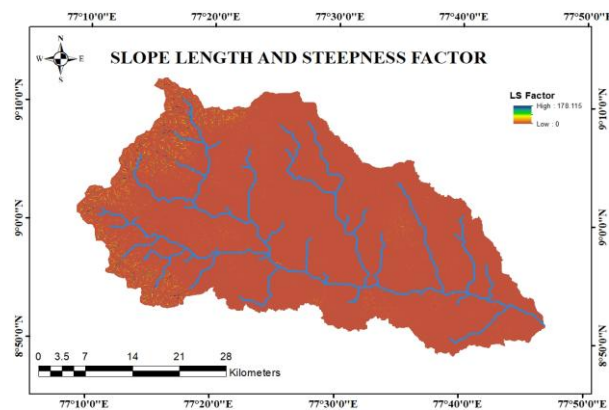


Figure 5. Slope length and steepness Factor Map

4.4 Cover management factor (C):

The C factor is a cover management is used to describe the effects of the land and crop management activities on soil erosion arised by water (Renard et al., 1997). C-factor Landuse/Landcover (LULC) data is usually used to calculate the C-factor and thus serves as the backbone of calculating this factor (Koirala et al., 2019). The cover management factor (C) in the basin ranges from 0.17 to 1.0, indicating a high degree of variability in land cover conditions and land-use practices. Higher C values, which correspond to sparse vegetation, bare soil, and poorly managed lands, are widely distributed across a significant portion of the basin, making these areas more vulnerable to soil erosion due to minimal surface protection against rainfall impact and runoff. In contrast, lower C values are limited to regions with dense vegetation cover, such as forested areas, plantations, and well-managed agricultural lands, where canopy cover and ground litter effectively reduce soil detachment and transport. This spatial distribution clearly demonstrates that land use and crop management practices play a crucial role in controlling soil erosion dynamics. Areas with intensive cultivation, fallow land, or degraded surfaces tend to exhibit higher erosion risk, whereas regions with sustainable vegetation cover and conservation practices show reduced susceptibility as Shown in Figure 6. Thus, the observed pattern underscores the importance of adopting improved land management strategies, and afforestation, to minimize erosion and enhance soil stability.

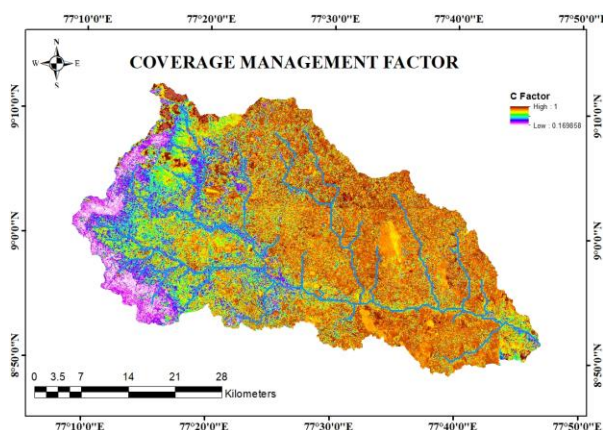


Figure 6. Coverage Management Factor Map.

4.5 Support practice factor (p):

he support practice factor (P-factor) is a crucial parameter in soil erosion assessment, representing the ratio of soil loss under specific conservation practices to that under standard upslope or downslope cultivation. It effectively reflects the impact of soil and water conservation measures in reducing erosion rates. In the present basin, the P-factor ranges from 0.4 to 1.0, indicating considerable spatial variability in the implementation and effectiveness of conservation practices. Lower P-values are associated with areas where effective mitigation measures such as contour farming, terracing, strip cropping, and bunding are practiced, significantly reducing surface runoff velocity and soil loss. Conversely, higher P-values are observed in regions with minimal or no conservation interventions, where traditional cultivation

practices dominate, leading to increased susceptibility to erosion. This spatial distribution highlights the critical role of conservation practices in controlling soil erosion and emphasizes the need for expanding and strengthening such measures, particularly in high-risk areas. The variation in P-factor, as depicted in Figure 7, provides valuable insight into the effectiveness of existing management strategies and helps identify priority zones for implementing improved soil and water conservation practices. Furthermore, enhancing conservation efforts in areas with high P-values can substantially reduce soil loss and improve long-term land productivity.

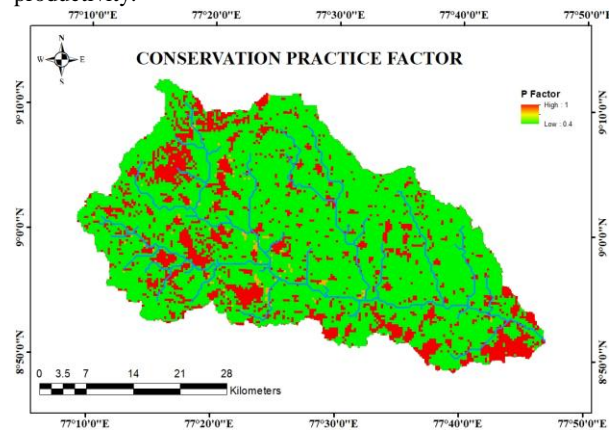


Figure 7. Coverage Management Factor Map

4.6 Average Annual soil loss:

The soil erosion map clearly indicates a distinct spatial variability in soil loss across the basin, with low erosion classes ($0-10 \text{ t ha}^{-1} \text{ yr}^{-1}$) dominating a major portion of the area. These regions are primarily associated with gentle slopes, well-structured and stable soils, and adequate vegetation cover that effectively reduces the impact of raindrop splash and surface runoff. In contrast, moderate erosion zones ($10-25 \text{ t ha}^{-1} \text{ yr}^{-1}$) are distributed intermittently, especially in transitional landscapes where variations in land use and topography begin to influence erosion dynamics. The high to very high erosion classes ($25-100 \text{ t ha}^{-1} \text{ yr}^{-1}$) are predominantly confined to steeper slopes, upper catchment areas, and along stream banks, where increased slope gradient and concentrated flow enhance runoff velocity and erosive power. Although extreme erosion zones ($>100 \text{ t ha}^{-1} \text{ yr}^{-1}$) occupy a relatively small spatial extent, they represent critical hotspots that demand immediate attention due to their potential to cause severe land degradation and sediment yield. The overall spatial pattern of soil erosion is controlled by the integrated effects of rainfall erosivity, slope characteristics, soil properties, land use/land cover, and existing conservation practices. Areas characterized by sparse vegetation and intensive agricultural activities are particularly vulnerable, as reduced ground cover and frequent soil disturbance accelerate detachment and transport processes. Furthermore, seasonal variability in rainfall, especially during peak monsoon periods, significantly amplifies erosion intensity in susceptible regions. Proximity to drainage networks further exacerbates the situation by facilitating efficient sediment transport, resulting in localized zones of high soil loss. These observations underscore the urgent need for implementing

site-specific soil and water conservation measures such as contour bunding, terracing, afforestation, and adoption of sustainable land management practices, which are essential to mitigate erosion risks, enhance land productivity, and ensure long-term environmental sustainability and soil management as illustrated in Figure 8.

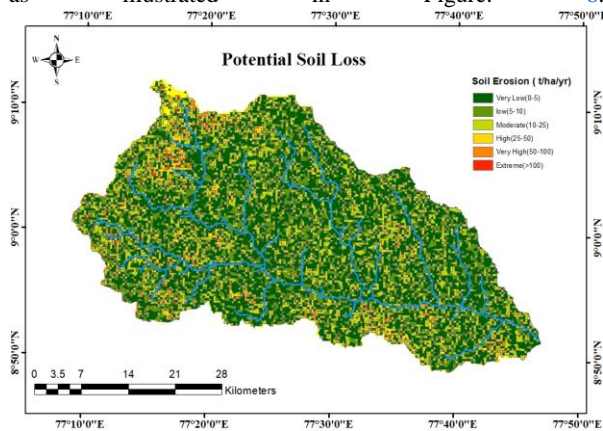


Figure 8. Potential Soil Erosion Map

5. Conclusion:

Based on the integrated RUSLE analysis, the basin exhibits clear spatial variability in soil erosion controlled by rainfall, soil properties, topography, land cover, and conservation management. The estimated annual soil loss reveals that most of the basin is very low erosion classes ($0\text{--}10\text{ t ha}^{-1}\text{ yr}^{-1}$), while moderate erosion ($10\text{--}25\text{ t ha}^{-1}\text{ yr}^{-1}$) occurs intermittently. Severe erosion zones ($25\text{--}100\text{ t ha}^{-1}\text{ yr}^{-1}$) and extreme erosion areas ($>100\text{ t ha}^{-1}\text{ yr}^{-1}$) are spatially limited but distinctly concentrated along steep slopes, upper catchment regions, and drainage networks, where high rainfall erosivity (R), slope length and steepness (LS), and cover-management (C) factors coincide with relatively lower conservation support (P) values, intensifying soil loss processes. These localized hotspots, though limited in spatial extent, contribute disproportionately to sediment yield and play a critical role in downstream sedimentation and land degradation. Furthermore, anthropogenic influences such as agricultural expansion, reduced vegetation cover, and improper land management practices further exacerbate erosion in these vulnerable zones. Therefore, these areas require immediate and priority-based soil and water conservation interventions, including contour bunding, terracing, afforestation, and improved land management strategies. Overall, the study demonstrates that the integration of the RUSLE model with Remote Sensing (RS) and Geographic Information Systems (GIS) provides a robust, reliable, and spatially explicit framework for quantifying soil erosion risk, identifying critical source areas, and supporting informed decision-making for sustainable watershed management and long-term environmental conservation.

Acknowledgements

The author expresses sincere and profound gratitude to the Director of the National Institute of Technology, Warangal, Telangana, India, for continuous guidance, encouragement, and unwavering institutional support throughout the course of this research, along with providing essential facilities and a conducive academic environment that played a pivotal role in the successful completion of this work. The author also

extends heartfelt appreciation to the faculty members, administrative staff, colleagues, and peers for their consistent cooperation, technical assistance, valuable suggestions, and constructive discussions, which significantly contributed to the progress, refinement, and overall quality of the study. Special acknowledgment is given for the availability of institutional resources, data support, and a collaborative research environment that facilitated the smooth execution of this work. Furthermore, the authors would like to sincerely thank the reviewers and the editorial team for their valuable time, insightful comments, constructive criticism, and expert suggestions, which have greatly enhanced the clarity, structure, scientific rigor, and overall presentation of this manuscript, ultimately strengthening its scientific contribution.

References:

- Aiello, A., Adamo, M., & Canora, F. (2015). Remote sensing and GIS to assess soil erosion with RUSLE3D and USPED at river basin scale in southern Italy. *CATENA*, 131, 174–185. <https://doi.org/10.1016/j.catena.2015.04.003>.
- Balasubramani, K., Veena, M., Kumaraswamy, K., Saravanabavan, V., 2015. Estimation of soil erosion in a semi-arid watershed of Tamil Nadu (India) using the revised universal soil loss equation (RUSLE) model through GIS. *Model Earth Syst. Environ.* 1,1–17. <http://doi.org/10.1007/s40808-015-0015-4>
- Beasley, D.B., Huggins, L.F., Monke, ampEJ, 1980. ANSWERS: a model for watershed planning. *Trans. ASAE* 23, 938–944.
- Devaraj, S., Sudalaimuthu, K. K., & Budamala, V. (2023).
- Dogra, Perna, Chiranjeev Kumawat, S. K. Goyal, and Omprakash. "Irrigation in India: status and challenges." (2022): 551-556.
- Ganasri B, Ramesh H. Assessment of soil erosion by RUSLE model using remote sensing and GIS - A case study of Nethravathi Basin. *Geoscience Frontiers*. 2016;7(6):953–961. <https://doi.org/10.1016/j.gsf.2015.10.007>
- Hui, L., Xiaoling, C., Lim, K. J., Xiaobin, C., & Sagong, M. (2010). Assessment of soil erosion and sediment yield in Liao watershed, Jiangxi Province, China, Using USLE, GIS, and RS. *Journal of Earth Science*, 21, 941–953. <https://doi.org/10.1007/s12583-010-0147-4>.
- Kayet, N., Pathak, K., Chakrabarty, A., Sahoo, S., 2018. Evaluation of soil loss estimation using the RUSLE model and SCS-CN method in hillslope mining areas. *Int. Soil and Water Conservation Res.* 6, 31–42.
- Kazamias, A.P., Sapountzis, M., Lagouvardos, K., 2017. Evaluation and intercomparison of GPM-IMERG and TRMM 3B42 daily precipitation products over Greece, in: Fifth International Conference on Remote Sensing and Geoinformation of the Environment (RSCy2017). International Society for Optics and Photonics, p. 1044413

Koirala, P., Thakuri, S., Joshi, S., Chauhan, R., 2019. Estimation of soil erosion in Nepal using a RUSLE modeling and geospatial tool. *Geosciences (Switzerland)* 9 <https://doi.org/10.3390/geosciences9040147>

Koirala, P., Thakuri, S., Joshi, S., Chauhan, R., 2019. Estimation of soil erosion in Nepal using a RUSLE modeling and geospatial tool. *Geosciences (Switzerland)* 9 <https://doi.org/10.3390/geosciences9040147>

Mohammed, J., & Mesapam, S. (2026). Performance evaluation of CMIP6 climate models for rainfall and erosivity in the thairabharani basin, India. *Theoretical and Applied Climatology*, 157(4), 189. <https://doi.org/10.1007/s00704-026-06071-8>

Mapping and assessing the spatial extent of floods using

Narayana, D.V.V., Babu, R., 1983. Estimation of soil erosion in India. *J. Irrig. Drain. Eng.*109, 419–434.

Pimentel, D., Harvey, C., Resosudarmo, P., Sinclair, K., Kurz, D., McNair, M., & Blair, R. (1995). Environmental and economic costs of soil erosion and conservation benefits. *Science*, 267(5201), 1117-1123. <https://doi.org/10.1126/science.267.5201.1117>

Pimentel, D., Harvey, C., Resosudarmo, P., Sinclair, K., Kurz, D., McNair, M., & Blair, R. (1995). Environmental and economic costs of soil erosion and conservation benefits. *Science*, 267(5201), 1117-1123. <https://doi.org/10.1126/science.267.5201.1117>

Renard K, Foster G, Weesies G, McCool D, Yoder D (1997) Predicting Soil Erosion by Water: A Guide to Conservation Planning with the RUSLE. US Department of Agriculture, Washington, DC.

Sentinel 1 SAR Data – An approach based on Flood Index

Shi ZH, Yan FL, Lu Li Li ZX, Cai CF. Interrill erosion from disturbed and undisturbed samples in relation to topsoil aggregate stability in red soils from subtropical China. *CATENA*.2010;81(3): 240-248. <https://doi.org/10.1016/j.catena.2010.04.007>

Tsegaye, L., Bharti, R. Soil erosion and sediment yield assessment using RUSLE and GIS-based approach in Anjeb watershed, Northwest Ethiopia. *SN Appl. Sci.* 3, 582 (2021). <https://doi.org/10.1007/s42452-021-04564-x>

Wischmeier, W. H., & Smith, D. D. (1978). Predicting rainfall erosion losses: a guide to conservation planning (No. 537). Department of Agriculture, Science and Education Administration.

Xiong, M., Sun, R., & Chen, L. (2019). A global comparison of soil erosion associated with land use and climate type. *Geoderma*, 343, 31-39. <https://doi.org/10.1016/j.geoderma.2019.02.013>.

Zhang, H., Renschler, C.S., Nichols, M.H., Nearing, M.A., 2021. Long-term, process-based, Continuous simulations for a small, nested rangeland watershed near Tombstone, AZ (USA): extending model validity to include soil redistribution. *Sci.Total Environ.* 792 <https://doi.org/10.1016/j.scitotenv.2021.148403>.